



Providing Choice & Value

Generic CT and MRI Contrast Agents



**FRESENIUS
KABI**

CONTACT REP

AJNR

**Reliable Initial Trauma CT Findings of
Supraclavicular Brachial Plexus Injury in
Patients Sustaining Blunt Injuries**

M.R. Povlow, J.R. Davis, A.M. Betts, S.M. Clayton, F.J.
Cloran, J.K. Aden and J.L. Ritter








This information is current as
of July 21, 2025.

AJNR Am J Neuroradiol 2023, 44 (8) 951-958

doi: <https://doi.org/10.3174/ajnr.A7919>

<http://www.ajnr.org/content/44/8/951>

Reliable Initial Trauma CT Findings of Supraclavicular Brachial Plexus Injury in Patients Sustaining Blunt Injuries

 M.R. Povlow,  J.R. Davis,  A.M. Betts,  S.M. Clayton,  F.J. Cloran,  J.K. Aden, and  J.L. Ritter



ABSTRACT

BACKGROUND AND PURPOSE: Traumatic brachial plexus injuries are uncommon but can be debilitating. Early diagnosis is critical. Most patients undergo CT after trauma. We sought to identify correlative CT findings of supraclavicular brachial plexus injuries to discern who may require further evaluation with MR imaging and to measure multireviewer performance for their interpretations.

MATERIALS AND METHODS: We identified all MR imaging examinations of the brachial plexus from our institution from January 2010 to January 2021 and included those performed for trauma. We excluded patients with penetrating or infraclavicular injuries and without preceding CTA of the neck or CT of the cervical spine. The cohort of 36 cases and 50 controls remained for analysis and were assessed for 6 findings: scalene muscle edema/enlargement, interscalene fat pad effacement, first rib fracture, cervical spine lateral mass/transverse process fracture, extra-axial cervical spinal hemorrhage, and cervical spinal cord eccentricity, forming a reference key. A resident physician and 2 neuroradiologists (blinded to the MR imaging) independently reviewed each CT scan for these findings. We measured agreement (Cohen κ) between observers and against the reference key.

RESULTS: Interscalene fat pad effacement (sensitivity, specificity, 94.44%, 90.00%; OR = 130.33; $P < .001$) and scalene muscle edema/enlargement (sensitivity, specificity, 94.44%, 88.00%; OR = 153.00; $P < .001$) correlated significantly with brachial plexus injury. Agreement between observers and the key was almost perfect for those findings and fractures (pooled $\kappa \geq 0.84$; $P < .001$). Agreement between observers was variable ($\kappa = 0.48$ – 0.97 ; $P < .001$).

CONCLUSIONS: CT can accurately predict brachial plexus injuries, potentially enabling earlier definitive evaluation. High interobserver agreement suggests that findings are consistently learned and applied.

ABBREVIATION: BPI = brachial plexus injuries

The brachial plexus is a complex neurologic structure in the neck and upper extremity supporting many functions (Fig 1). Brachial plexus injuries (BPI) are uncommon injuries in patients affected by trauma, occurring in about 1%.¹ Common causative mechanisms include traction on the head and neck such as in vehicular collisions (particularly motorcycles and snowmobiles) and

penetrating trauma in cases of stabbings or shootings.¹ BPI may be classified by the varying degrees of damage to the nerves and nervous system supporting structures,² initially based on the work by Sunderland³ and Seddon,⁴ and these degrees of damage carry important prognostic information.⁵ The site of injury is clinically important because supraclavicular injuries, especially preganglionic rootlet avulsions, are the most grave.^{1,6} Other factors including diagnostic delay and delayed referral for surgical repair, both increasing the time from injury to repair, have also shown significant detriment to functional recovery.⁷


Diagnostic imaging, as a noninvasive complement to surgical exploration, has become critical in evaluating patients with suspected BPI. The evolution of optimal imaging assessment for BPI dramatically occurred across time, beginning with conventional radiographs and myelography, followed by CT myelography, and currently rests at MR imaging of the brachial plexus as the criterion standard in an attempt to accurately detect the location of injury.^{8–11} CT without myelography lacks the superior soft-tissue contrast resolution of MR imaging and historically has not been used to evaluate BPI.² It

Received July 24, 2022; accepted after revision May 31, 2023.

From the Department of Radiology (M.R.P., J.R.D., A.M.B., S.M.C., F.J.C., J.L.R.), and United States Army Graduate Medical Education (J.K.A.), Joint Base San Antonio–Fort Sam Houston, San Antonio, Texas.

The views expressed herein are those of the author(s) and do not necessarily reflect the official policy or position of the Defense Health Agency, Brooke Army Medical Center, the Department of Defense, nor any agencies under the U.S. Government.

Please address correspondence to Michael R. Povlow, MD, Department of Radiology, Brooke Army Medical Center, 3551 Roger Brooke Dr, Joint Base San Antonio–Fort Sam Houston, San Antonio, TX 78234; e-mail: michael.r.povlow.mil@health.mil

 Indicates open access to non-subscribers at www.ajnr.org

 Indicates article with online supplemental data.

<http://dx.doi.org/10.3174/ajnr.A7919>

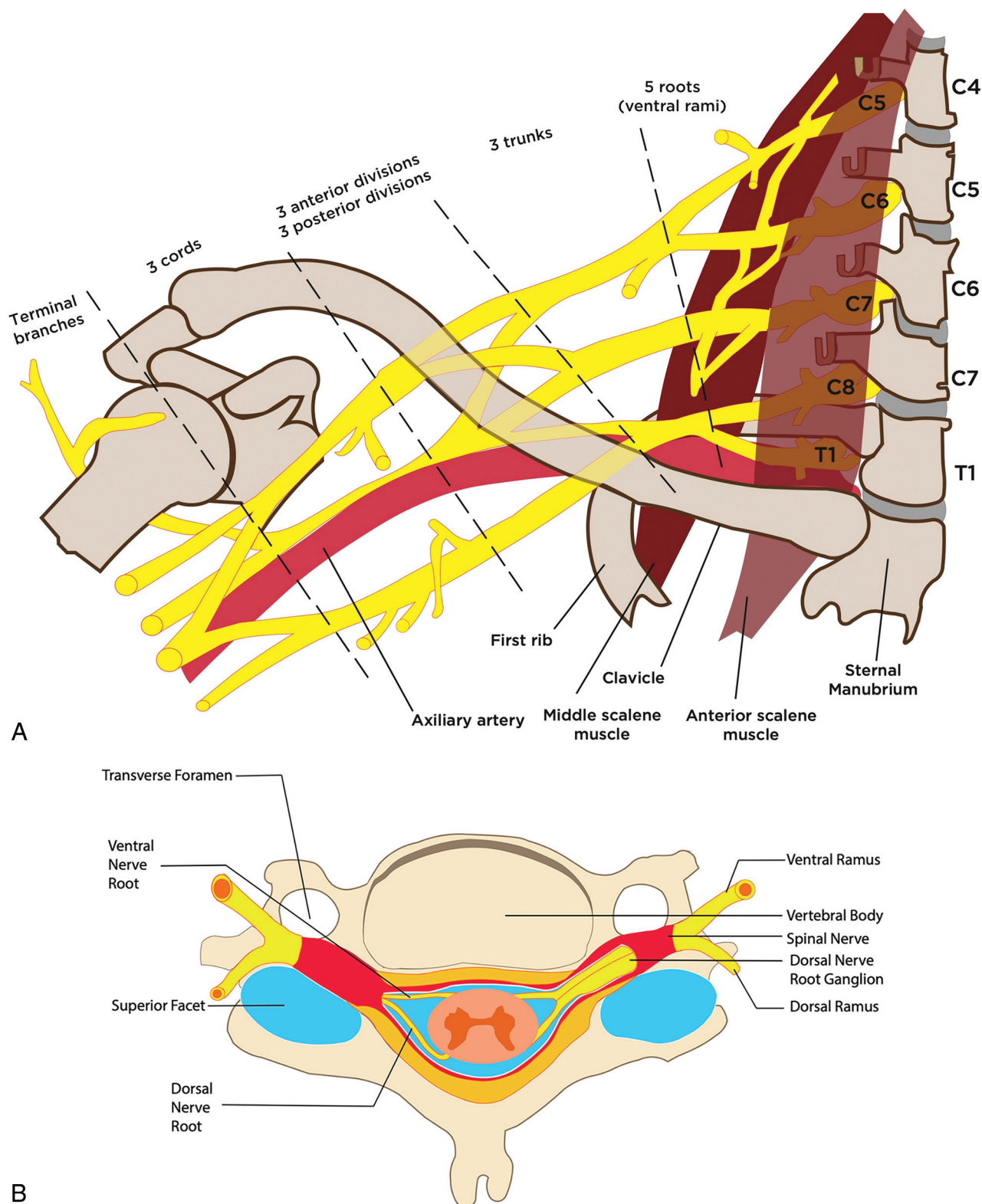


FIG 1. Anatomy of the brachial plexus. A frontal illustration (A) shows the anatomy of the brachial plexus as it arises from the neural foramina from the C4 to T1 levels, coursing between the anterior and middle scalene muscles and giving rise to many nerve branches. The cervical nerve roots of the brachial plexus are numbered 1 higher than the level where they originate (eg, the C5 nerve root arises from the C4 level, the C6 root from the C5 level, and so forth) because the C1 nerve root arises from above the C1 vertebral body at the skull base, and subsequently, there is a C8 nerve root but not a C8 vertebral body. The brachial plexus is divided into 5 roots, 3 trunks, 6 divisions, 3 cords, and terminal branches. A cross-sectional illustration (B) shows the anatomy of the proximal portions of the brachial plexus and nerve rootlets as they exit the spinal cord. Fibers from the dorsal rootlet complex with first-order sensory nerves in the dorsal root ganglion and fibers from both ventral and nerve rootlets blend before separating into ventral and dorsal nerve rami outside the neural foramina. The ventral rami go on to become the roots of the brachial plexus.

is, however, often performed for initial trauma evaluation and may detect the first signs of a traumatic lesion in this sensitive area.²

The objectives of this retrospective study are 2-fold. First, we aimed to establish the diagnostic utility of traumatic findings of BPI on CT by identifying injuries and injury patterns on the initial CT imaging in a cohort of patients with subsequent MR imaging performed for concern for BPI, thereby enabling radiologists to predict the presence of BPI on the basis of the initial trauma CT scan earlier in the hospital course. If successful, this process enables earlier definitive imaging and surgical treatment or, in the case of a nonsurgical injury, early physical therapy for prevention of long-term morbidity. Second, we aimed to evaluate

the interobserver agreement between a resident physician and 2 fellowship-trained neuroradiologists when evaluating these findings, with the end goal of extrapolating the validity and generalizability that might be expected in various practice environments.

MATERIALS AND METHODS

Given that this is a retrospective study, our local human research protections office declared the study to be human subjects research exempt from institutional research board and associated regulatory requirements. The Health Insurance Portability and Accountability Act (HIPAA) regulations applied, but given the retrospective analysis, a waiver of HIPAA authorization was approved. Data were kept in compliance with all HIPAA standards.

Our 2-part retrospective reader-based diagnostic performance study began with a retrospective search for all consecutive brachial plexus MR imaging examinations performed at our level 1 trauma center from January 2010 through January 2021 (Table 1), which was performed using our hospital's PACS. The inclusion criterion for our cohort was to have undergone MR imaging for brachial plexus evaluation. Following exclusion of MR imaging examinations performed for nontraumatic reasons, MR imaging examinations were then separated into groups by whether they were interpreted as positive or negative for BPI. Any examination initially interpreted as indeterminate was independently reviewed by a fellowship-trained neuroradiologist (J.L.R., with a 2-year neuro-radiology fellowship and 14 years of postfellowship experience), and a final determination was made. Examinations were excluded if they were not performed for the evaluation of trauma (Fig 2).

Any examination that included a penetrating or infraclavicular injury (ie, inferior to the clavicle) was excluded. We then reviewed the imaging performed before MR imaging, and patients who did not undergo an initial evaluation with either CT neck angiography or CT of the cervical spine without contrast for evaluation of traumatic injuries (within 48 hours of injury) were excluded. CT myelograms were not included in this study because they neither reflect the criterion standard nor are typically used in initial polytrauma imaging.

Imaging Parameters

The protocol and imaging parameters for the MR imaging of the brachial plexus, CT of the cervical spine, and the CT neck angiography varied during 11 years, but the most common protocol and ranges are the following:

1. MR imaging of the brachial plexus examination included a large-FOV coronal STIR of the bilateral brachial plexus as well as 3-plane spin-echo 2D oblique imaging along the

Table 1: Patient demographics and mechanisms of injury by case group

Characteristic	Cases (n = 36)	Controls (n = 50)
Age (range) (mean) (yr)	18–75 (38.7)	18–73 (41.5)
Sex		
Male	29	36
Female	7	14
Mechanism of injury		
Motor vehicle collision	26	25
Motorcycle collision	5	1
Fall from height ^a	3	8
All-terrain vehicle accident	2	0
Motor vehicle vs pedestrian	0	7
Assault	0	4
Fall from standing	0	3
Fall from horse	0	1
Bicycle accident	0	1

^a Fall from height = (>10 ft, 3.048 m).

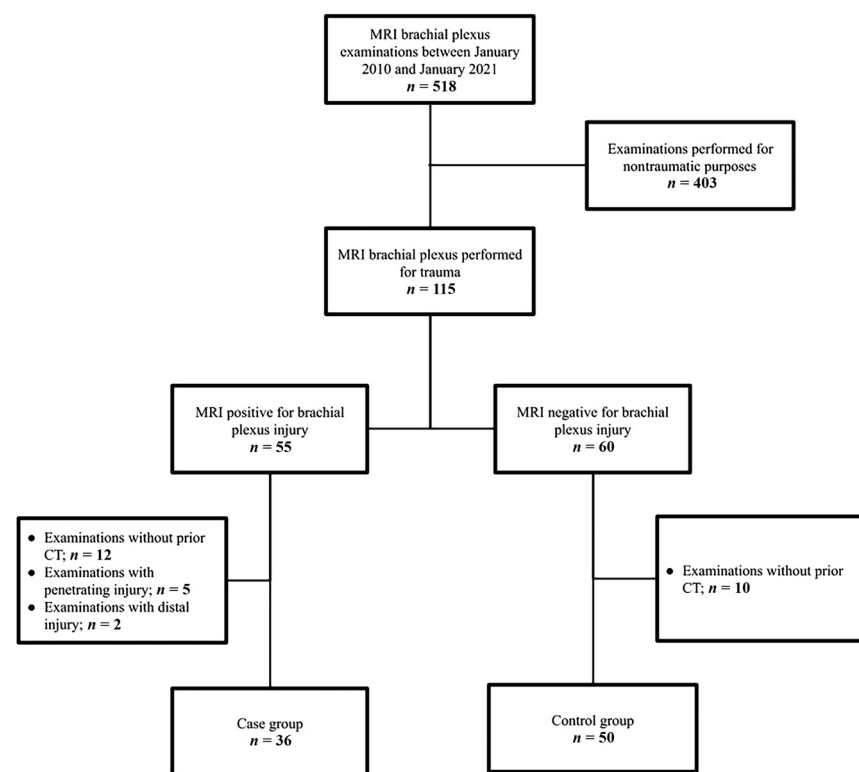


FIG 2. Inclusion and exclusion criteria. A flowchart delineates the inclusion and exclusion criteria used in this study, resulting in a case group of 36 and a control group of 50.

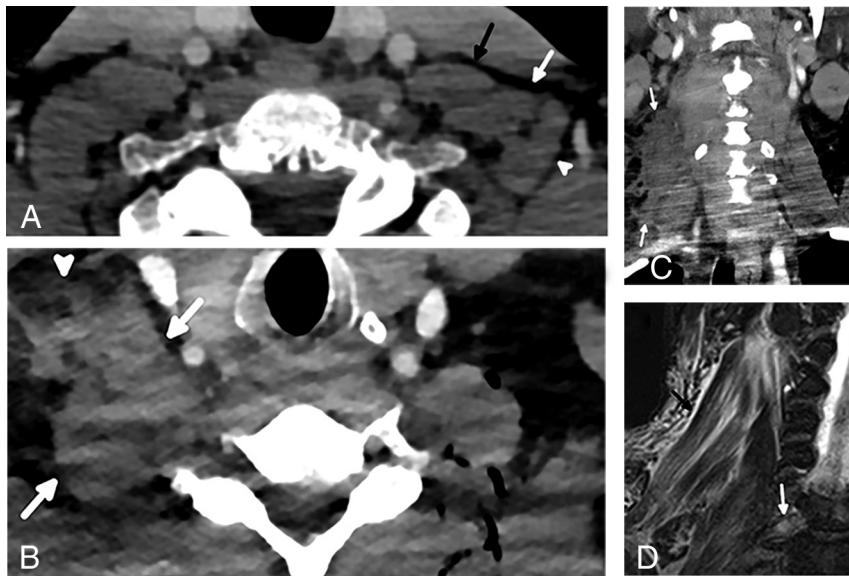


FIG 3. Normal and abnormal scalene muscles in different patients. An axial CT image in a 48-year-old man (A) without BPI shows normal anterior (black arrow), middle (white arrow), and posterior (arrowhead) scalene muscles without enlargement or edema. An axial CT image in a 52-year-old man (B) with BPI shows enlargement of the right scalene muscles (arrows) with extensive surrounding edema (arrowhead). A coronal CT image in the same patient (C) shows the extent of the asymmetric edema (arrows). A coronal T2 STIR MR imaging performed a day later in the 52-year-old patient (D) again shows scalene enlargement and edema (black arrow). Thickening and signal hyperintensity within the right C7 root (white arrow) are consistent with a stretch injury; similar findings were present at other levels.

course of the side of clinical concern in both T1 and STIR. The T1 images were acquired with a TR range of 566–700 ms and a TE range of 9–10 ms. The STIR images were acquired with a TR range of 2500–2600 ms and a TE range of 75–76 ms. Also performed were axial oblique 3D volumetric acquired spoiled gradient-echo sequences with a TR of 15 ms, a TE of 5 ms, and a flip angle of 28°.

2. The CT cervical spine examination was performed at 120 kV (peak) using dose-modulation acquisition techniques. Slice thicknesses were 2 mm and acquired in the axial plane. Three-plane sharpened bone kernel images were provided as were axial and sagittal planes in a smooth soft-tissue kernel.
3. The CT neck angiography examinations were performed at 120 kVp and used dose-modulation acquisition techniques. Slice thickness was 1 mm and was acquired in the axial plane using a smooth soft-tissue kernel with coronal and sagittal reformats. Patients received 100 mL of iodine-based IV contrast of iodixanol, 320 mg/mL (Visipaque; GE Healthcare).

Reference Standard

For the first portion of our study, a resident physician (M.R.P., postgraduate year 4) and the senior author (J.L.R.) evaluated all CT examinations for the presence of 6 specific findings, which were predetermined on the basis of a prior, smaller-scale retrospective abstract:¹² scalene muscle edema/enlargement (Fig 3), interscalene fat pad effacement (Fig 4), first-rib fracture, cervical spine lateral mass or transverse process fracture, extra-axial cervical spinal hemorrhage (Fig 5), and cervical spinal cord eccentricity (Fig 6). Before determining the presence or absence of these

findings, the study orders were randomized and the demographic information was hidden. These results were tabulated and used as the reference key against which observers would be measured during the second portion of the study. We determined the sensitivity, specificity, and OR of these findings with 95% CIs when compared with the presence or absence of BPI on the MR imaging examination.

Agreement Compared with the Reference Key and between Observers

For the second portion of our study, a separate resident physician (J.R.D., postgraduate year 5) and 2 separate fellowship-trained neuroradiologists (A.M.B., 2-year neuroradiology fellowship and 7 years of postfellowship experience; S.M.C., 1-year neuroradiology fellowship and 3 years of postfellowship experience) underwent individual 15-minute training sessions led by the first author, which detailed positive and negative examples of CT findings from cases outside the study cohort. The examinations

were de-identified, and the readers then independently reviewed each CT examination, blinded to the results of the MR imaging or neurologically localizing information, and determined whether the 6 CT findings were present or absent on each examination, interpreted in a specific order sorted by examination date. The observers were able to use all images provided in the examination, including multiplanar reformats and reconstruction kernels (eg, bone, soft-tissue) if they were performed at the time of the initial imaging acquisition, and all standard tools available in the PACS (eg, window width and level adjustment, sharpening and softening filters). If the patient had undergone both a CT of the cervical spine and CT neck angiography, the observers were provided with the CT neck angiogram because the overall data provided (eg, a larger FOV, improved soft-tissue contrast resolution) were better on this examination. Interobserver agreement (Cohen κ) for each reviewer was compared against the reference key generated in the first portion of the study, as well as against the other reviewers. Pooled interobserver agreement (Cohen κ) was calculated from the individual reviewer's data by determining a two-thirds majority (ie, when ≥ 2 of the 3 reviewers determined a finding present or absent when evaluated independently), which was compared with the reference key for the presence or absence of each finding.

All statistical analyses were performed using JMP, Version 13.2 (SAS Institute) by a professional statistician (J.K.A.). Significance for statistical tests was set at $P < .05$. κ statistics were appraised as to their level of agreement on the basis of prior work by Landis and Koch:¹³ $\kappa < 0.00$, "poor"; $\kappa = 0.00$ –0.20, "slight"; $\kappa = 0.21$ –0.40, "fair"; $\kappa = 0.41$ –0.60, "moderate"; $\kappa = 0.61$ –0.80, "substantial"; $\kappa = 0.81$ –1.00, "almost perfect."

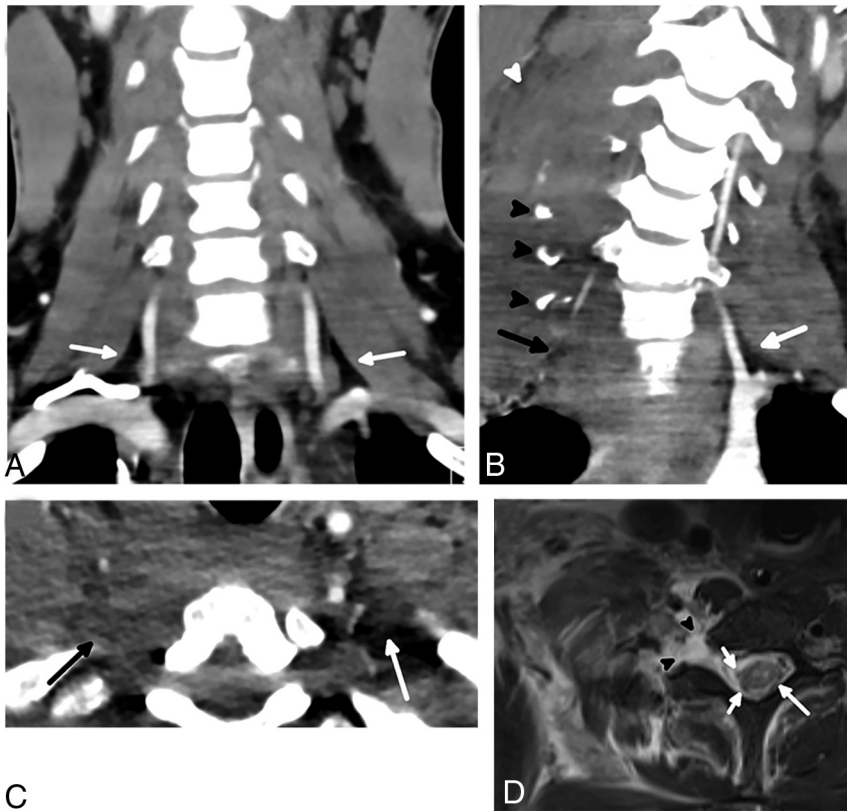


FIG 4. Normal and abnormal interscalene fat pads in different patients. A coronal CT scan in a 26-year-old man (A) without BPI demonstrates smoothly margined scalene muscles with normal interscalene fat pad (arrows). The coronal plane is a good place to assess the interscalene fat pad quickly by looking for this triangle of fat in the region of the proximal vertebral arteries, which should not have any stranding or hematoma. A coronal CT scan in a 25-year-old man (B) with BPI shows complete effacement of the right interscalene fat pad (black arrow) compared with the normal left interscalene fat pad (white arrow). Multiple displaced cervical transverse process fractures (black arrowheads) with scalene enlargement and edema (white arrowhead) are also present. An axial CT in the 25-year-old patient (C) shows the interscalene fat pad effacement (black arrow) in a different plane, compared with the normal left interscalene fat pad (white arrow). An axial T2-weighted MR imaging with fat saturation (D) performed a day later in the injured patient shows avulsion of the ventral and dorsal nerve rootlets (short white arrows), which was better appreciated when reviewing multiple sequential images. The spinal cord is slightly eccentric to the left and has abnormally increased signal (long white arrow), most pronounced within the gray matter. A large pseudomeningocele is present (arrowheads).

RESULTS

A total of 518 brachial plexus MR imaging examinations were reviewed (Fig 2), of which 403 were excluded because they were not performed for evaluating a traumatic injury. Of the 115 remaining examinations, 55 were positive for BPI and 60 were negative for BPI, constituting the cases and controls. There were 2 positive examinations that demonstrated infraclavicular BPI and 5 with penetrating trauma, so they were excluded from further analysis. Another 12 examinations were excluded from the case group and 10 from the control group because they did not have an initial CT of the cervical spine or CT neck angiography. A total of 36 cases and 50 controls remained for analysis. The spectrum of injuries found on the MR imaging examinations of the brachial plexus included nerve rootlet avulsion, nerve rupture, and neuropraxia, all occurring within the supraclavicular brachial plexus. The range of time between initial CT imaging and MR imaging of the brachial plexus spanned 24 hours to 9 months.

were highest for first-rib fractures, where they were almost perfect (0.84–0.93, $P < .001$). Agreement was also almost perfect between readers 1 and 2 for cervical lateral mass/transverse process fracture (0.86, $P < .001$). Spinal cord eccentricity had moderate agreement between all reader pairs (0.48–0.59, $P < .001$), and scalene muscle edema/enlargement had moderate agreement between readers 1 and 2 and 1 and 3 (0.49 and 0.59, $P < .001$). Agreement for the remaining findings was substantial for all reader pairs (0.64–0.74, $P < .001$).

DISCUSSION

Of the 6 CT findings, scalene muscle edema/enlargement and interscalene fat pad effacement were most strongly associated with BPI and demonstrated good sensitivity and specificity. This has a sound anatomic basis because the brachial plexus runs through the interscalene fat pad between the anterior and middle scalenes, and damage to one structure may risk damage to the

Reference Standard

Scalene muscle edema/enlargement and interscalene fat pad effacement were both 94.44% (95% CI, 81.86%–98.46%) sensitive for BPI with specificities of 88.00% (95% CI, 76.19%–94.38%) and 90.00% (95% CI, 78.64%–95.65%), respectively (Table 2). Of the remaining 4 findings, cervical lateral mass/transverse process fracture was most sensitive, 55.56% (95% CI, 39.58%–70.46%) and spinal cord eccentricity was least sensitive, 13.89% (95% CI, 6.08%–28.66%); however, all findings were specific in this cohort, ranging from 86.00% to 100.00%. Except for spinal cord eccentricity, each finding was significantly associated with BPI (OR = 3.91–153.00, $P \leq .01$).

Agreement Compared with the Reference Key and between Observers

Pooled κ statistics from all reviewers compared with the reference key were substantial or almost perfect for all findings (0.77–0.94, $P < .001$) and were highest for first-rib and cervical lateral mass/transverse process fractures (Online Supplemental Data). Except for spinal cord eccentricity, individual κ statistics compared with the reference key were also substantial or almost perfect (0.65–0.97, $P < .001$) and highest for fractures. For spinal cord eccentricity, the individual κ statistics were moderate for reviewers 1 and 2 (0.59 and 0.48, $P < .001$) and substantial for reviewer 3 (0.79, $P < .001$).

Individual κ statistics between reviewers

other. Interobserver agreement for these findings was particularly strong between the neuroradiologists, despite the subjectivity that is inherent to the evaluation of the soft tissues on CT. While the brachial plexus itself is not as well-characterized in detail on CT as on MR imaging, evidence of damage to these intimately adjacent structures acts as a valid surrogate marker for BPI. In the

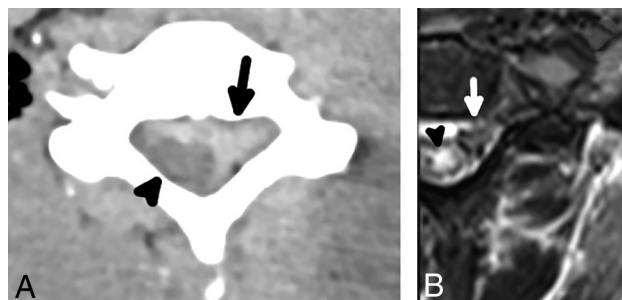


FIG 5. A 42-year-old man with preganglionic BPI and extra-axial hemorrhage. An axial CT image (A) shows a large extra-axial hematoma centered at the left of the spinal canal (arrow), which appears to compress the eccentric spinal cord (arrowhead). An axial T2 STIR MR imaging (B) in the same patient performed a day later shows an extra-axial hematoma (arrow); the hematoma and motion artifacts on the examination limit the diagnostic quality, but multilevel nerve rootlet avulsions are evident on sequential images. There is also severely abnormal signal hyperintensity (arrowhead) and a probable focus of hemorrhage (focal T2 hypointensity) in the spinal cord.

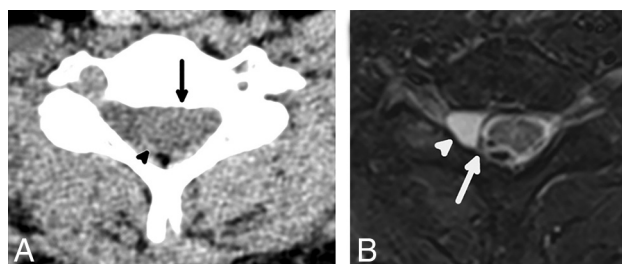


FIG 6. A 26-year-old man with preganglionic BPI and eccentricity of the spinal cord. An axial CT image (A) shows subtle eccentricity of the spinal cord and thecal sac (arrow) with an asymmetric amount of CSF in the right aspect of the spinal canal, which is indicative of a pseudomeningocele. There is also thin extra-axial hemorrhage (arrowhead) along the posterior aspect of the spinal cord. An axial T2 STIR MR imaging performed a day later in the same patient (B) shows complete avulsion of the ventral and dorsal nerve rootlets with eccentricity of the spinal cord (arrow), which is lateralized to the left of the spinal canal, compatible with preganglionic BPI. A small pseudomeningocele is confirmed on MR imaging (arrowhead) and is a finding highly associated with nerve rootlet avulsion.

case of interscalene fat pad effacement, this notion is concordant with previous assumptions that a hematoma in the interscalene fat pad is highly suspicious for BPI.² Scalene muscle edema and enlargement are evident when there is fat stranding adjacent to the scalenes or visible enlargement of the muscle bodies (Fig 3) and can be quickly assessed on axial and coronal images. Interscalene fat pad effacement also typically manifests with fat stranding or frank hematoma, and we found that this was most easily and quickly assessed by scrutinizing the fat adjacent to the proximal vertebral arteries on coronal images (Fig 4), though this region can and should also be assessed on other multiplanar images. Both findings are best assessed with a soft-tissue reconstruction kernel, possibly making its routine addition to a trauma CT cervical spine examination valuable.

First-rib and cervical lateral mass/transverse process fractures are injuries that indicate high-energy trauma with a vector that overlaps the brachial plexus. The scalene muscles, between which the brachial plexus courses, originate at the transverse processes of C2 through C7, and the anterior and middle scalenes insert on the first rib. Abrupt and forceful lateral flexion of the neck may cause traction and result in avulsion of the contralateral scalene muscles and has been postulated to be the primary cause of cervical transverse process fractures;¹⁴ this may also account for a proportion of first-rib fractures for the same reason. Such traction on the neck has also been associated with BPI,¹ and it has been reported that as many as 10% of patients with cervical transverse process fractures may have concomitant BPI.¹⁵ We found that both findings were specific in this cohort for and significantly associated with BPI. This finding is concordant with prior literature and also supports the assumption, based on the anatomy, that scalene muscle injury is closely associated with BPI. Fracture detection is already part of a standard trauma search pattern, and in keeping with this notion, we found interobserver agreement to be excellent and the highest of all CT findings. However, because fractures are a common finding in polytrauma, caution must be used when raising the suspicion for BPI if no other specific findings are present.

Extra-axial spinal canal hemorrhage manifests on CT as hyperattenuating products outside the spinal cord and can be identified when sought. While larger amounts of hemorrhage may be most readily identified, subtle cases with smaller hemorrhages can be challenging to visualize on CT compared with MR imaging, which is extremely sensitive to blood products. This issue is, in part, due to the lower contrast resolution of CT and the proximity to osseous structures, which can prevent selection of an optimal window width and level setting. Spinal cord eccentricity is also a subtle finding on CT, which can be difficult to

Table 2: Prevalence, sensitivities, specificities, and ORs of the CT findings

Finding	Cases (n = 36)	Controls (n = 50)	Sensitivity (95% CI)	Specificity (95% CI)	OR, P Value (95% CI)
Scalene muscle edema/enlargement	34	6	94.44 (81.86–98.46)	88.00 (76.19–94.38)	130.33; $P < .001$ (24.77–685.87)
Interscalene fat pad effacement	34	5	94.44 (81.86–98.46)	90.00 (78.64–95.65)	153.00; $P < .001$ (27.97–836.89)
First-rib fracture	14	7	38.89 (24.78–55.14)	86.00 (73.81–93.05)	3.91; $P = .01$ (1.38–11.09)
Cervical lateral mass or transverse process fracture	20	4	55.56 (39.58–70.46)	92.00 (81.16–96.85)	14.38; $P < .001$ (4.27–48.45)
Extra-axial spinal canal hemorrhage	10	0	27.78 (15.85–43.99)	100.00 (92.86–100)	40.02; $P = .01$ (2.26–709.90)
Spinal cord eccentricity	5	0	13.89 (6.08–28.66)	100.00 (92.86–100)	17.63; $P = .05$ (0.9425–329.97)

identify prospectively because differences in patient positioning and the close similarities in the attenuation of the spinal cord compared with the adjacent CSF are likely to result in lower precision. Coupled with the low prevalence of these findings in our cohort, we favor that these imaging subtleties were the reasons that sensitivity was low compared with the other findings. Spinal cord eccentricity was also the only finding that was not significantly associated with BPI in this cohort, possibly also relating to its low prevalence. On the other hand, extra-axial spinal canal hemorrhage and spinal cord eccentricity were 100% specific for BPI in this cohort, and we suggest that when present, they indicate severe injury that correlates more highly with nerve rootlet avulsion in the same manner as a pseudomeningocele, both of which may be better appreciated on MR imaging or a CT myelogram.^{2,6,8,16} Caution should be exercised in the use of extra-axial hemorrhage within the cervical spine as a predictor of brachial plexus injury because extra-axial intracranial hemorrhage as well as vertebral fractures may also lead to spinal canal hemorrhage.

With κ analysis of the CT findings, pooled and individual statistics showed that agreement was substantial or near-perfect with the exception of spinal cord eccentricity. This result may be, in part, because of the difficulty in identifying the contents of the spinal canal. In regard to interobserver κ statistics, the analysis showed that agreement was most consistently high between the 2 neuroradiologists for denoting the presence of scalene muscle edema/enlargement and interscalene fat pad effacement, likely due to similar levels of expertise and consistency.

There were limitations to our study design. There was selection bias because CT examinations were chosen for analysis only if the MR imaging had been performed later to assess for BPI. Doing so does not take into account all patients undergoing CT neck angiography or CT of the cervical spine for trauma; therefore, the authors could not determine whether the findings presented may be equally or more prevalent in situations in which there is no clinical concern for BPI. Clinical concern for BPI also increases the pretest probability of finding BPI and abnormal findings on CT. The readers, while blinded to the results of the MR imaging, still implicitly expected that there would be a higher-than-normal number of cases positive for BPI in the study cohort due to this increased pretest probability. Subsequently, it is possible that detection of the CT findings may have been subject to a degree of bias that would not be present for a radiologist interpreting unknown cases in his or her normal practice.

Finally, this was a single-institution study, which may limit its overall generalizability. However, given our diverse patient population, this is thought to be less of a concern, and experiences would likely be comparable at other level 1 trauma centers. A future prospective trial with a larger cohort would be warranted to determine whether these findings would be valid with inclusion of all patients with CT neck angiography and cervical spine CT after their traumatic episode and would mitigate selection bias.

There were also minor limitations in image quality and examination protocols due to varied examination practices during an 11-year period on multiple scanners. For example, given the

traditional CT neck angiography or cervical spine protocol at our institution, the complete extent of the first rib was not always seen, and while first-rib fracture was ultimately a finding of secondary importance, it could still limit performance and utility in some cases. Streak artifacts from contrast within the vascular system or from the upper extremities at times obscured visualization of the structures at the base of the neck. Finally, soft-tissue reconstructions were only variably present on cervical spine CT examinations, limiting evaluation of the most significant CT findings of BPI, namely scalene muscle edema/enlargement and interscalene fat pad effacement.

Despite these limitations and MR imaging is ubiquitous in major medical centers, identification of possible BPI at the time of initial CT trauma imaging has a potential impact in multiple scenarios. In the setting of a patient who is under general anesthesia or comatose at the time of initial imaging and cannot participate in a neurologic examination, concerning CT findings may prompt further imaging and specialist consultation. Also, small community hospitals, stand-alone emergency rooms, and urgent care clinics in the United States may have CT as their most advanced cross-sectional resource; identification of possible BPI may lead to more prompt disposition and transfer of the patient. Furthermore, in the situation of locales in underprivileged countries or hospitals established in austere environments overseas, BPI identification on CT may lead to prompt transfer to a higher level of care. Ultimately, identifying these potential high-yield findings on CT may advance radiologists' ability to care for patients in a broad spectrum of environments.

CONCLUSIONS

Assessment of initial CT neck angiography or cervical spine imaging performed for the work-up of traumatic injury can predict which patients are at risk of BPI and which patients may benefit from early MR imaging of the brachial plexus. In particular, scalene muscle edema/enlargement and interscalene fat pad effacement correlate highly and can be quickly incorporated into an existing trauma search pattern. However, because MR imaging remains the imaging criterion standard for detecting and describing BPI, negative or equivocal CT findings should not prevent further evaluation in patients with suspicious clinical findings or a high-risk mechanism of injury. We also found substantial or almost perfect interobserver agreement on all findings when comparing the reference key and the resident physician and neuroradiologist observers, despite the subjectivity and subtlety of some of the findings. While we found that interobserver agreement for single findings between readers was more variable, agreement was still good for key findings like scalene muscle edema/enlargement and interscalene fat pad effacement. This finding suggests that these results are relatively straightforward and accessible, allowing radiologists with varying levels of comfort with neurotrauma imaging to successfully apply this knowledge in standard practice. We suggest that knowledge of these high-value findings is important to any radiologist who routinely interprets trauma imaging and may potentially decrease costly delays in care for patients with BPI.

ACKNOWLEDGMENT

The authors would like to thank Mr Ernesto Menchaca for his diligent work and patience in providing our medical illustrations.

Disclosure forms provided by the authors are available with the full text and PDF of this article at www.ajnr.org.

REFERENCES

1. Midha R. **Epidemiology of brachial plexus injuries in a multitrauma population.** *Neurosurgery* 1997;40:1182–89 [CrossRef Medline](#)
2. Gilcrease-Garcia BM, Deshmukh SD, Parsons MS. **Anatomy, imaging, and pathologic conditions of the brachial plexus.** *Radiographics* 2020;40:1686–714 [CrossRef Medline](#)
3. Sunderland S. **A classification of peripheral nerve injuries producing loss of function.** *Brain* 1951;74:491–516 [CrossRef Medline](#)
4. Seddon HJ. **Three types of nerve injury.** *Brain* 1943;66:237–88 [CrossRef](#)
5. Singer AD, Meals C, Kesner V, et al. **The multidisciplinary approach to the diagnosis and management of nonobstetric traumatic brachial plexus injuries.** *AJR Am J Roentgenol* 2018;211:1319–31 [CrossRef Medline](#)
6. Wade RG, Takwoingi Y, Wormald JCR, et al. **MRI for detecting root avulsions in traumatic adult brachial plexus injuries: a systematic review and meta-analysis of diagnostic accuracy.** *Radiology* 2019;293:125–33 [CrossRef Medline](#)
7. Martin E, Senders JT, DiRisio AC, et al. **Timing of surgery in traumatic brachial plexus injury: a systematic review.** *J Neurosurg* 2019;130:1333–45 [CrossRef](#)
8. Doi K, Otsuka K, Okamoto Y, et al. **Cervical nerve root avulsion in brachial plexus injuries: magnetic resonance imaging classification and comparison with myelography and computerized tomography myelography.** *J Neurosurg* 2002;96:277–84 [CrossRef Medline](#)
9. Walker AT, Chaloupka JC, de Lotbiniere AC, et al. **Detection of nerve rootlet avulsion on CT myelography in patients with birth palsy and brachial plexus injury after trauma.** *AJR Am J Roentgenol* 1996;167:1283–87 [CrossRef Medline](#)
10. Gad DM, Hussein MT, Omar NN, et al. **Role of MRI in the diagnosis of adult traumatic and obstetric brachial plexus injury compared to intraoperative findings.** *Egypt Journal of Radiology and Nuclear Medicine* 2020;51:195 [CrossRef](#)
11. Takahara T, Hendrikse J, Yamashita T, et al. **Diffusion-weighted MR neurography of the brachial plexus: feasibility study.** *Radiology* 2008;249:653–60 [CrossRef Medline](#)
12. Tharin B, Kini J, York G, et al. **Traumatic Brachial Plexus Injuries: Retrospective Review of Findings on Presenting CT Evaluation.** Presented at: American Society of Emergency Radiology (ASER) 23rd Annual Meeting, September 14, 2011. Key Biscayne, Florida
13. Landis JR, Koch GG. **The measurement of observer agreement for categorical data.** *Biometrics* 1977;33:159–74 [CrossRef Medline](#)
14. Newell N, Pearce AP, Spurrier E, et al. **Analysis of isolated transverse process fractures sustained during blast-related events.** *J Trauma Acute Care Surg* 2018;85:S129–33 [CrossRef Medline](#)
15. Woodring JH, Lee C, Duncan V. **Transverse process fractures of the cervical vertebrae: are they insignificant?** *J Trauma* 1993;34:797–802 [CrossRef Medline](#)
16. Yoshikawa T, Hayashi N, Yamamoto S, et al. **Brachial plexus injury: clinical manifestations, conventional imaging findings, and the latest imaging techniques.** *Radiographics* 2006;26:S133–43 [CrossRef Medline](#)